¹H-N.m.r. study of enzymically generated wheat-endosperm arabinoxylan oligosaccharides: structures of hepta- to tetradeca-saccharides containing two or three branched xylose residues

Rainer A. Hoffmann, Theo Geijtenbeek, Johannis P. Kamerling, and Johannes F. G. Vliegenthart*

Bijvoet Center, Department of Bio-Organic Chemistry, Utrecht University, P.O. Box 80.075, 3508 TB Utrecht (The Netherlands)

ABSTRACT

The structures of hepta- to tetradeca-saccharides, generated by digestion of wheat-endosperm arabinoxylan with endo-(1→4)-β-D-xylanase, and isolated by gel-permeation chromatography on Bio-Gel P-6 and high-performance anion-exchange chromatography with pulsed amperometric detection (h.p.a.e.–p.a.d.), were elucidated using monosaccharide and methylation analysis, f.a.b.-m.s., and ¹H-n.m.r. spectroscopy. The structures identified had two branching elements, →4)[α-L-Araf-(1→3)]-β-D-Xylp-(1→ and/or →4)[α-L-Araf-(1→2)][α-L-Araf-(1→3)]-β-D-Xylp-(1→, directly connected to each other in all four possible combinations. The h.p.a.e.–p.a.d. elution pattern showed that these combinations are not present in equal amounts. Also, compounds containing two 2,3-branched β-D-Xylp residues separated by one or two unbranched β-D-Xylp residues were found, and the presence of a tetradecasaccharide containing three 2,3-branched β-D-Xylp residues was established.

INTRODUCTION

Wheat-endosperm arabinoxylans consist of a (1→4)-linked β-D-Xylp backbone with unsubstituted, and 3- and 2,3-substituted β-D-Xylp residues in various ratios, with mainly single α-L-Araf groups attached[1,2]. So far, little information is available about the distribution of the α-L-Araf substituents along the xylan backbone. Periodate-oxidation studies of intact arabinoxylans have indicated the occurrence of clusters of branched β-D-Xylp residues, up to xylotetraose elements[1,3].

Recently, we reported[4] the isolation and ¹H-n.m.r. characterisation (2D HOHA-HA and 2D ROESY) of penta- to hepta-arabinoxylan oligosaccharides containing single 3- and 2,3-branched β-D-Xylp residues, obtained by digestion of wheat arabinoxylan with an *Aspergillus* endo-(1→4)-β-D-xylanase. We now report the elucidation of the structure of larger arabinoxylan oligosaccharides isolated from the digest, containing two to three branching units in various combinations, and discuss the specificity of the applied xylanase.

---

* To whom correspondence should be addressed.

EXPERIMENTAL

Preparation of arabinoxylan oligosaccharides. — Arabinoxylan oligosaccharides were generated by an *Aspergillus* endo-$(1\rightarrow4)$-β-D-xylanase digestion[4] of an arabinoxylan (L-PP$_{44}$), isolated from the tailing fraction of the white flour of the soft wheat variety Kadet[2]. The mixture of oligosaccharides was fractionated on a column (100 × 2.5 cm) of Bio-Gel P-6 (200–400 mesh, Bio-Rad) as described[4]. The Bio-Gel P-6 fractions **4, 5,** and **6** were fractionated further by high-performance anion-exchange chromatography with pulsed amperometric detection (h.p.a.e.–p.a.d.) on a Dionex Bio-LC system consisting of a quaternary gradient pump, a model PAD-2 detector, and a CarboPac PA-1 pellicular anion-exchange resin column (250 × 9.0 mm)[4]. Detection by p.a.d. with a gold working electrode and triple-pulse amperometry[5] comprised the following pulse potentials and durations: E$_1$ 0.05 V, 300 ms; E$_2$ 0.65 V, 120 ms; E$_3$ − 0.95 V, 60 ms; and a response time of 1 s. Samples were dissolved in H$_2$O (500 μL) and applied in five 100-μL portions. Separations were carried out with aqueous NaOH, using a concentration gradient of NaOAc at 4 mL/min and ambient temperature; specific conditions are included in the legend of Fig. 2. Fractions were neutralised immediately with M HCl, lyophilised, desalted on a column (60 × 1 cm) of Bio-Gel P-2 (200–400 mesh, Bio-Rad), passed through a column (10 × 0.5 cm) of Dowex 50W-X8 (H$^+$) resin (100–200 mesh, Bio-Rad) at 4°, and lyophilised. If necessary, Dionex fractions were subfractionated at a lower molarity of aqueous NaOH and a different concentration gradient of NaOAc (see legend of Fig. 2).

Monosaccharide analysis. — Samples (0.1 mg) were methanolysed (methanolic M HCl, 24 h, 85°) and the resulting methyl glycosides were analysed by g.l.c. of the trimethylsilylated derivatives[6,7] on an SE-30 fused-silica capillary column (25 m × 0.32 mm, Pierce), using a Varian 3700 gas chromatograph connected to a Shimadzu C-R3A recorder/integrator.

Methylation analysis. — Samples (0.2 mg) were reduced with NaBD$_4$ (10 mg) in water (2 mL) for 16 h at ambient temperature, the pH was adjusted to 4 by the addition of Dowex 50W-X8 (H$^+$) resin (100–200 mesh) at 4°, and the solution was filtered and lyophilised. Boric acid was removed by evaporation of methanol from the residue under reduced pressure. Methylation analysis of the resulting oligosaccharide-alditols was performed as described[8]. Partially methylated alditol acetates were analysed by g.l.c. on a CPsil 43 WCOT fused-silica capillary column (25 m × 0.32 mm, Chrompack), and by g.l.c.–m.s. on a Carlo–Erba GC/Kratos MS 80/Kratos DS 55 system (electron energy, 70 eV; accelerating voltage, 2.7 kV; ionising current, 100 μA; CPsil 43 capillary column).

^{1}H-N.m.r. spectroscopy. — Samples were repeatedly treated with D$_2$O (99.9 atom % D, MSD Isotopes), finally using 99.96 atom % D at pD ≥ 7. Resolution-enhanced 600-MHz ^{1}H-n.m.r. spectra were recorded with a Bruker AM-600 spectrometer (SON-hf-NMR facility, Department of Biophysical Chemistry, Nijmegen University), operating at a probe temperature of 27°. Chemical shifts (δ) are expressed in p.p.m. downfield from the signal for internal sodium 4,4-dimethyl-4-silapentane-1-sulfonate (DSS), but were actually measured by reference to internal acetone (δ 2.225 in D$_2$O at 27°)[9] with an accuracy of 0.002 p.p.m.

Homonuclear Hartmann–Hahn (HOHAHA) spin-lock experiments were recorded using the pulse sequence, $90°-t_1-SL-acq^{10-13}$, where SL stands for a multiple of the MLEV-17 sequence. The spin-lock field strength corresponded to a 90° pulse width of 27 μs and a total spin-lock mixing time of 105 ms. The spectral width was 2994 Hz in each dimension.

Rotating-frame n.O.e. spectroscopy (ROESY) involved the pulse sequence, $90_\varphi°-t_1-SL-acq^{14}$, where SL stands for a continuous spin-lock pulse of 200 ms at a field strength corresponding to a 90° pulse width between 112 and 120 μs. The carrier frequency was placed at the left side of the spectrum at 5.7 p.p.m. in order to minimise HOHAHA-type magnetisation transfer. The HOD signal was suppressed by presaturation during 1.0 s. The spectral width was 3205 Hz in each dimension.

For both HOHAHA and ROESY spectra, 512 experiments of 4K data points were recorded. The time-proportional phase-increment method (TPPI)[15] was used to create t_1 amplitude modulation. The data matrixes were zero-filled to 1K × 8K and multiplied in each time domain with a phase-shifted sine function, shifted $\pi/3$ for the HOHAHA and $\pi/2$ for the ROESY, prior to phase-sensitive F.t.

RESULTS

The mixture of oligosaccharides, generated by digestion of wheat arabinoxylan with endo-(1→4)-β-D-xylanase, was fractionated on Bio-Gel P-6 (Fig. 1), and fractions 1–3 have been discussed[4]. Fractions 4 and 5, containing oligosaccharides composed of 7 to 11 monosaccharides (see below), were subfractionated by h.p.a.e.–p.a.d. (Figs. 2A and 2B), yielding 8 main fractions, 34, 41, 51, 54, 56, 57, 58, and 59. Further fractionation of 54 and 57 by h.p.a.e.–p.a.d., under different conditions, afforded 54.1–54.3 (Fig. 2C) and 57.1–57.2 (Fig. 2D), respectively. Fraction 54.1 was too complex for further analysis. H.p.a.e.–p.a.d. of Bio-Gel P-6 fraction 6 gave a major peak 60 (data not shown), corresponding with an oligosaccharide composed of 14 monosaccharides (see below). The structural data for the various fractions, except 34 and 51, obtained from positive-ion f.a.b.-m.s. and monosaccharide analysis, are presented in Table I, and those from methylation analysis in Table II. The oligosaccharide(s) in 41 contained xylopentaose cores with two internal Xylp residues 3-substituted by single Araf residues. The oligosaccharides in 54.3 and 56 also contained xylopentaose cores, but with two internal Xylp residues 3- and 2,3-substituted by single Araf residues. The same substitution pattern holds for the oligosaccharide(s) present in 54.2, having xylohexaose cores. Furthermore, the oligosaccharides in 57.1, 57.2, 58, and 59 are composed of xylopentaose to xyloheptaose cores with two internal Xylp residues 2,3-substituted by single Araf residues. Fraction 60 contained an oligosaccharide with a xylo-octaose core, with three internal Xylp residues 2,3-substituted by single Araf residues. The primary structures of these oligosaccharides were elucidated further by ¹H-n.m.r. spectroscopy.

As shown by ¹H-n.m.r. spectroscopy (data not presented), fraction 51 contained a mixture of oligosaccharides with internal Xylp residues solely 3-substituted. A subfractionation of 51 by h.p.a.e.–p.a.d. did not lead to fractions of sufficient purity to be
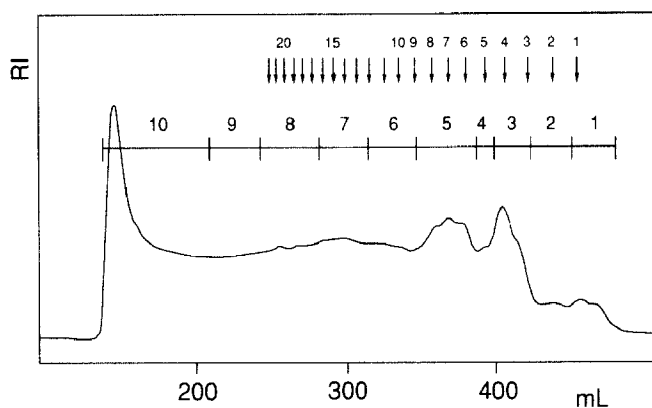
Fig. 1. Bio-Gel P-6 elution profile of oligosaccharides obtained by incubation of arabinoxylan with endo-$(1\rightarrow4)$-β-D-xylanase. The arrows at the top indicate the elution position of gluco-oligosaccharides generated by the hydrolysis of dextran, and the associated numbers indicate the d.p.

TABLE I

Monosaccharide analysis data of h.p.a.e.-p.a.d. fractions derived from Bio-Gel P-6 fractions **4**, **5**, and **6**, together with the mol. mass and number of pentose units (in parentheses) of the major component present, as determined by positive-ion f.a.b.-m.s.

Monosaccharides[a]	Fraction								
	41	**54.2**	**54.3**	**56**	**57.1**	**57.2**	**58**	**59**	**60**
Ara	2.0	3.0	3.0	3.0	4.0	4.0	4.0	4.0	6.0
Xyl	5.1	6.0	5.0	5.4	6.9	6.0	6.0	5.6	8.2
Mol. mass	942	1206	1074	1074	1470	1338	1338	1206	1866
	(7)	(9)	(8)	(8)	(11)	(10)	(10)	(9)	(14)

[a] Expressed as molar ratios relative to Ara.

TABLE II

Methylation analysis data of h.p.a.e.-p.a.d. fractions derived from Bio-Gel P-6 fractions **4**, **5**, and **6**

Alditol acetate	Molar ratio						
	41	**54**	**56**	**57**	**58**	**59**	**60**
2,3,5-Me$_3$-Ara[a,b]	1.1	1.3	1.0	1.6	2.2	2.4	4.2
1,2,3,5-Me$_4$-Xyl[b]	0.2	0.1	0.2	0.4	0.3	0.2	0.3
2,3,4-Me$_3$-Xyl[b]	0.5	0.4	0.3	0.4	0.6	0.6	0.5
2,3-Me$_2$-Xyl	0.9	1.2	1.2	2.2	1.9	1.2	2.9
2-Me-Xyl	2.0[c]	1.0[c]	1.0[c]	–	–	+	+
Xyl	–	0.9	0.9	2.0[c]	2.0[c]	2.0[c]	3.0[c]

[a] 2,3,5-Me$_3$-Ara = 1,4-di-O-acetyl-2,3,5-tri-O-methylarabinitol, *etc.* [b] Because of the relatively high volatility of these residues, these values are lower than expected. [c] Taken as 1.0, 2.0, or 3.0.
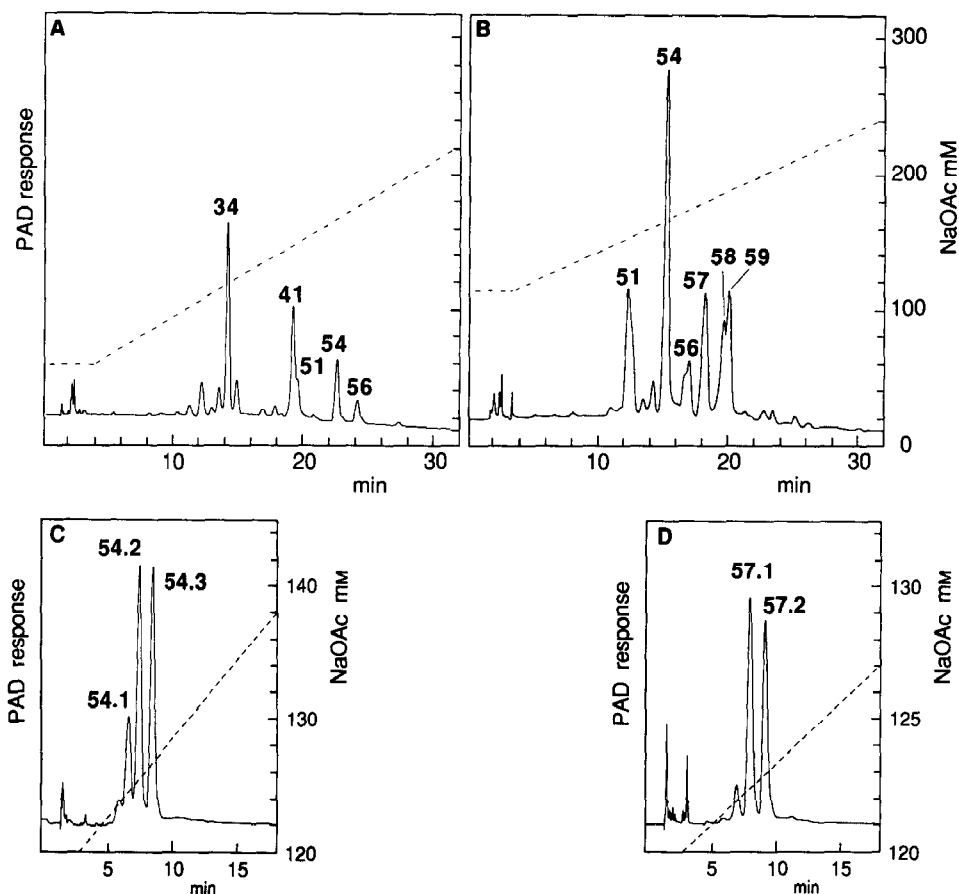
Fig. 2. H.p.a.e.–p.a.d. fractionation patterns of Bio-Gel P-6 fractions 4 (A) and 5 (B) and of the h.p.a.e.–p.a.d. fractions 54 (C) and 57 (D) on a CarboPac PA-1 column. The column was eluted with a linear concentration gradient (------) from (A) 60–260mM NaOAc in 0.1M NaOH during 35 min, (B) 110–270mM NaOAc in 0.1M NaOH during 35 min, (C) 120–160mM NaOAc in 35mM NaOH during 20 min, (D) 120–130mM NaOAc in 35mM NaOH during 20 min. Fractions were collected as indicated.

characterised. The presence of fraction 34 in Bio-Gel P-6 fraction 4 stems from overlap of fractions 4 and 3, and the oligosaccharides in 34 have been reported in relation to Bio-Gel P-6 fraction 3 (ref. 4).

Fraction 41. — The intensities of the signals for anomeric protons in the ¹H-n.m.r. spectrum of 41 (Fig. 3) pointed to the presence of a single diarabinosylxylopentaose, AX-41, with the Xyl$p$ residues β ($J_{1,2}$ 7–8 Hz) and the Ara$f$ residues α ($J_{1,2} \sim 1$ Hz)[16]. On the various H-1 tracks of the constituent monosaccharides in the 2D HOHAHA spectrum (Fig. 4), the total scalar-coupled networks of each residue were observed, and the data obtained are summarised in Table III. Specific assignment of the α-Ara$f$ H-5$proR$,5$proS$ signals is based on their relative chemical shifts ($\delta_{5proR} > \delta_{5proS}$), supported by the $J_{4,5}$ values ($J_{4,5proR} < J_{4,5proS}$)[17]. Part of the ROESY spectrum, containing the sequence information, is presented in Fig. 5, and the observed n.O.e.'s along the H-1

tracks are compiled in Table IV. The n.O.e.'s between H-1 of β-Xyl$p$-(**n**) and H-4,5eq of β-Xyl$p$-(**n − 1**), together with the connectivities α-Ara$f$-A^{3X3} H-1,β-Xyl$p$-3^{II} H-3 and α-Ara$f$-A^{3X4} H-1,β-Xyl$p$-4^{II} H-3 established the sequence of **AX-41**.

Comparison of the spectral data for **AX-41** with those of reference compound **AX-31** [β-Xyl$p$-4-(α-Ara$f$-A^{3X3})β-Xyl$p$-3^{II}-β-Xyl$p$-2-Xyl$p$-1][4] shows nearly identical sets of chemical shifts for β-Xyl$p$-1,2,3^{II}. The proton resonances of the terminal β-Xyl$p$-4^{II},5 element in **AX-41** show upfield shifts, as compared to the same element in reference compound **AX-32a** [β-Xyl$p$-5-(α-Ara$f$-A^{3X4})β-Xyl$p$-4^{II}-β-Xyl$p$-3-β-Xyl$p$-2-Xyl$p$-1][4], missing α-Ara$f$-A^{3X3}.

Fraction **54.3**. — The intensities of the signals for anomeric protons in the ^{1}H-n.m.r. spectrum of **54.3** (Fig. 6A) indicated[16] the presence of a single triarabinosyl-xylopentaose, **AX-54c**. In the 2D HOHAHA spectrum of the non-subfractionated fraction **54** (not shown), on the various H-1 tracks of the constituent monosaccharides belonging to the major compound **AX-54c**, the total scalar-coupled networks of each
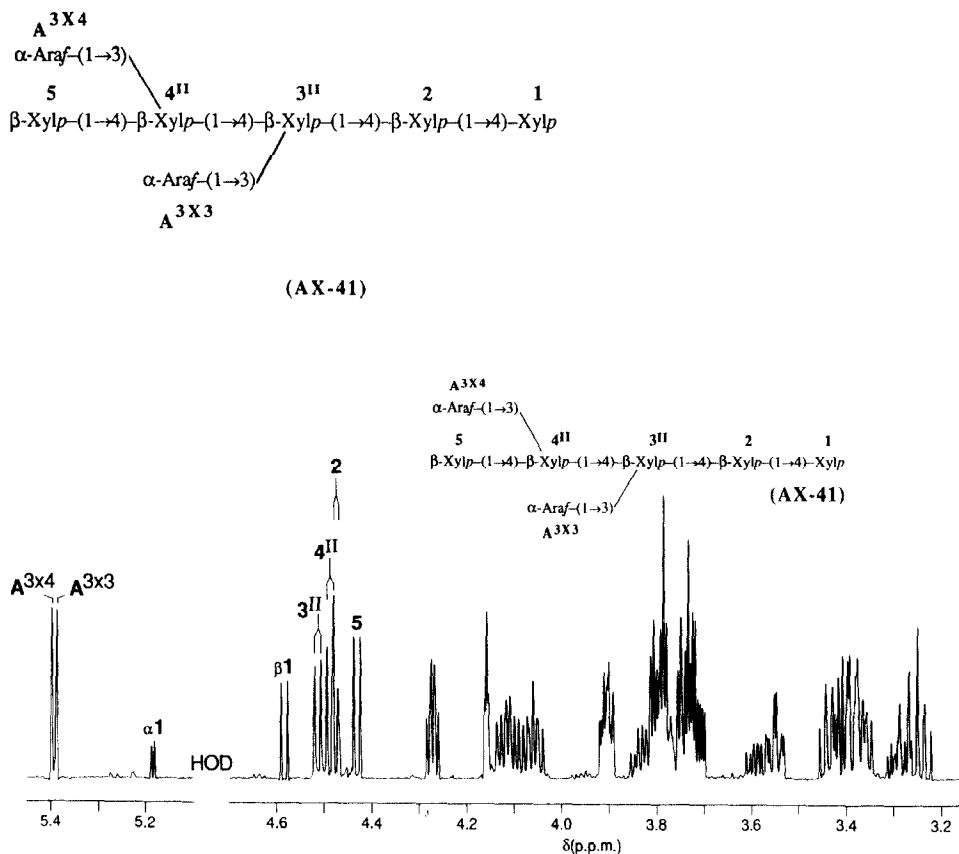

Fig. 3. Resolution-enhanced 600-MHz ^{1}H-n.m.r. spectrum of fraction **41**. The numbers and letters in the spectrum refer to the corresponding residues in the structure.

TABLE III

[1]H-N.m.r. data for the arabinoxylan hepta- to tetradeca-oligosaccharides derived from enzymically degraded wheat arabinoxylan

Compound[a]	Residue[b]	Chemical shift[c]					
		H-1	H-2	H-3	H-4	H-5eq/ H-5proR	H-5ax/ H-5proS
AX-41	α-Xylp-1	5.184	3.545			—3.73–3.82—	
	β-Xylp-1	4.584	3.249	3.547	3.779	4.055	3.379
	β-Xylp-2$_\alpha$	4.474	3.301				
	β-Xylp-2$_\beta$	4.472	3.292	3.552	3.793	4.105	3.376
	β-Xylp-2$_\beta$	4.477	3.292				
	β-Xylp-3[II]	4.514	3.442	3.741	3.837	4.124	3.400
	β-Xylp-4[II]	4.488	3.430	3.735	3.793	4.068	3.366
	β-Xylp-5	4.431	3.236	3.408	3.592	3.907	3.270
	α-Araf-A[3X3]	5.388	4.162	3.911	4.273	3.801	3.720
	α-Araf-A[3X4]	5.398	4.158	3.900	4.273	3.795	3.715
AX-54c	α-Xylp-1	5.183	3.545			—3.73–3.82—	
	β-Xylp-1	4.584	3.249	3.546	3.772	4.053	3.378
	β-Xylp-2$_\alpha$	4.465	3.299				
				3.562	3.792	4.143	3.417
	β-Xylp-2$_\beta$	4.467	3.290				
	β-Xylp-3[III]	4.637	3.570	3.825	3.878	4.142	3.429
	β-Xylp-4[II]	4.480	3.439	3.738[d]	3.792	4.078	3.361
	β-Xylp-5	4.435	3.238	3.409	3.592	3.908	3.267
	α-Araf-A[2X3]	5.225	4.150	3.959	4.128	3.819	3.722
	α-Araf-A[3X3]	5.271	4.166	3.939	4.304	3.801	3.726
	α-Araf-A[3X4]	5.402	4.159	3.902	4.275	3.795	3.716
AX-54b	α-Xylp-1	5.183	3.545			—3.73–3.82—	
	β-Xylp-1	4.584	3.249	3.546	3.772	4.053	3.378
	β-Xylp-2	4.467	3.290	3.562	3.792	4.143	3.417
	β-Xylp-3[III]	4.637	3.570	3.825	3.878	4.142	3.429
	β-Xylp-4[II]	4.481	3.439	3.733[d]	3.792	4.078	3.361
	β-Xylp-5	4.453	3.270	3.533	3.759	4.045	3.334
	β-Xylp-6	4.448	3.247	3.421·	3.621	3.965	3.299
	α-Araf-A[2X3]	5.225	4.150	3.959	4.128	3.819	3.722
	α-Araf-A[3X3]	5.270	4.166	3.939	4.304	3.801	3.726
	α-Araf-A[3X4]	5.396	4.160	3.910	4.273	3.799·	3.719
AX-56	α-Xylp-1	5.184	3.544			—3.73–3.82—	
	β-Xylp-1	4.584	3.248	3.546	3.778	4.054	3.378
	β-Xylp-2$_\alpha$	4.474	3.298				
				3.551	3.780	4.100	3.373
	β-Xylp-2$_\beta$	4.477	3.290				
	β-Xylp-3[II]	4.501	3.440	3.762	3.834	4.139	3.462
	β-Xylp-4[III]	4.595	3.558	3.80	3.81	4.082	3.382
	β-Xylp-5	4.425	3.244	3.410	3.594	3.915	3.267
	α-Araf-A[3X3]	5.419	4.162	3.920	4.304	3.820	3.732
	α-Araf-A[2X4]	5.231	4.146	3.975	4.147	3.838	3.744
	α-Araf-A[3X4]	5.274	4.165	3.931	4.310	3.792	3.720

TABLE III (continued)

Compound[a]	Residue[b]	Chemical shift[c]					
		H-1	H-2	H-3	H-4	H-5eq/ H-5proR	H-5ax/ H-5proS
AX-59	α-Xylp-1	5.184	3.544	——————3.73–3.82——————			
	β-Xylp-1	4.584	3.248	3.546	3.773	4.052	3.377
	β-Xylp-2$_\alpha$	4.464	3.296	3.558	3.784	4.141	3.416
	β-Xylp-2$_\beta$	4.467	3.289				
	β-Xylp-3^{III}	4.629	3.566	3.86	3.87	4.142	3.502
	β-Xylp-4^{III}	4.579	3.568	3.80	3.81	4.088	3.369
	β-Xylp-5	4.429	3.244	3.411	3.596	3.917	3.267
	α-Araf-A^{2X3}	5.222	4.152	3.958	4.126	3.818	3.721
	α-Araf-A^{3X3}	5.294	4.166	3.946	4.334	3.834	3.743
	α-Araf-A^{2X4}	5.243	4.148	3.976	4.166	3.838	3.738
	α-Araf-A^{3X4}	5.282	4.166	3.933	4.314	3.794	3.723
AX-58a	α-Xylp-1	5.183	3.544	——————3.73–3.82——————			
	β-Xylp-1	4.584	3.248	3.546	3.771	4.051	3.377
	β-Xylp-2	4.478	3.288	3.552	3.783	4.102	3.375
	β-Xylp-3	4.471	3.289	3.559	3.783	4.139	3.416
	β-Xylp-4^{III}	4.628	3.565	3.86	3.87	4.143	3.498
	β-Xylp-5^{III}	4.578	3.568	3.80	3.81	4.087	3.368
	β-Xylp-6	4.429	3.244	3.411	3.596	3.917	3.267
	α-Araf-A^{2X4}	5.221	4.152	3.958	4.127	3.817	3.721
	α-Araf-A^{3X4}	5.294	4.166	3.945	4.333	3.833	3.742
	α-Araf-A^{2X5}	5.242	4.148	3.976	4.166	3.837	3.738
	α-Araf-A^{3X5}	5.281	4.167	3.933	4.314	3.794	3.722
AX-58b	α-Xylp-1	5.183	3.544	——————3.73–3.82——————			
	β-Xylp-1	4.584	3.248	3.546	3.771	4.051	3.377
	β-Xylp-2	4.467	3.289	3.559	3.783	4.139	3.416
	β-Xylp-3^{III}	4.628	3.565	3.86	3.87	4.143	3.498
	β-Xylp-4^{III}	4.578	3.568	3.80	3.81	4.087	3.368
	β-Xylp-5	4.445	3.276	3.535	3.750	4.056	3.329
	β-Xylp-6	4.450	3.248	3.421	3.621	3.966	3.297
	α-Araf-A^{2X3}	5.221	4.152	3.958	4.127	3.817	3.721
	α-Araf-A^{3X3}	5.294	4.166	3.945	4.333	3.833	3.742
	α-Araf-A^{2X4}	5.242	4.148	3.976	4.166	3.837	3.738
	α-Araf-A^{3X4}	5.281	4.167	3.940	4.314	3.797	3.726
AX-57a	α-Xylp-1	5.183	3.545	——————3.73–3.82——————			
	β-Xylp-1	4.584	3.248	3.545	3.772	4.051	3.377
	β-Xylp-2$_\alpha$	4.465	3.298	3.560	3.792	4.143	3.417
	β-Xylp-2$_\beta$	4.468	3.291				
	β-Xylp-3^{III}	4.639	3.570	3.825	3.870	4.140	3.430
	β-Xylp-4	4.443	3.285	3.550	3.758	4.099	3.379
	β-Xylp-5^{III}	4.628	3.564	3.825	3.870	4.140	3.421
	β-Xylp-6	4.436	3.254	3.417	3.600	3.921	3.274
	α-Araf-A^{2X3}	5.224	4.149	3.958	4.128	3.817	3.720
	α-Araf-A^{3X3e}	5.271	4.165	3.939	4.305	3.799	3.725
	α-Araf-A^{2X5}	5.221	4.144	3.954	4.128	3.817	3.720
	α-Araf-A^{3X5e}	5.271	4.165	3.933	4.305	3.795	3.722

TABLE III (continued)

Compound[a]	Residue[b]	Chemical shift[c]					
		H-1	H-2	H-3	H-4	H-5eq/ H-5proR	H-5ax/ H-5proS
AX-57b	α-Xylp-1	5.183	3.547	————3.73–3.82————			
	β-Xylp-1	4.584	3.248	3.546	3.772	4.052	3.377
	β-Xylp-2$_\alpha$	4.465	3.298				
	β-Xylp-2$_\beta$	4.468	3.291	3.560	3.792	4.140	3.417
	β-Xylp-3^{III} = 6^{III}	4.639	3.569	3.828	3.871	4.142	3.430
	β-Xylp-4	4.454	3.286	3.543	3.752	4.058	3.340
	β-Xylp-5	4.463	3.286	3.557	3.792	4.140	3.408
	β-Xylp-7	4.436	3.254	3.418	3.600	3.922	3.276
	α-Araf-A$^{2[X3,X6]}$	5.226	4.149	3.959	4.127	3.817	3.720
	α-Araf-A$^{3[X3,X6]}$	5.273	4.166	3.939	4.305	3.797	3.725
AX-60	α-Xylp-1	5.183	3.545	————3.73–3.82————			
	β-Xylp-1	4.584	3.248	3.546	3.773	4.051	3.376
	β-Xylp-2	4.467	3.290	3.557	3.782	4.139	3.416
	β-Xylp-3^{III}	4.627	3.564	3.86	3.87	4.142	3.503
	β-Xylp-4^{III}	4.578	3.568	3.80	3.81	4.086	3.369
	β-Xylp-5	4.445	3.277	3.536	3.747	4.053	3.331
	β-Xylp-6	4.462	3.290	3.557	3.782	4.139	3.416
	β-Xylp-7^{III}	4.638	3.569	3.828	3.873	4.142	3.432
	β-Xylp-8	4.436	3.254	3.418	3.602	3.922	3.274
	α-Araf-A^{2X3}	5.221	4.151	3.958	4.126	3.817	3.720
	α-Araf-A^{3X3}	5.293	4.165	3.944	4.331	3.831	3.740
	α-Araf-A^{2X4}	5.243	4.147	3.975	4.165	3.837	3.737
	α-Araf-A^{3X4}	5.280	4.165	3.938	4.314	3.796	3.724
	α-Araf-A^{2X7}	5.225	4.150	3.958	4.125	3.817	3.720
	α-Araf-A^{3X7}	5.273	4.165	3.938	4.304	3.796	3.723

[a] Compounds are represented by short-hand symbolic notation: ●, Xylp; ◇ α-Araf; ●–●β-Xylp-(1→4)-Xylp; α-Araf-(1→2)-β-Xylp; α-Araf-(1→3)-β-Xylp. [b] The Xylp residue in the reducing position is denoted **1**, etc.; **2**$_{\alpha/\beta}$ means reducing Xylp-1 residue in α/β configuration (anomerisation effect). Araf-A^{2X3} means arabinofuranose linked to O-2 of Xylp-3, etc.; Xylp-3^{I} means Xylp-3 branched at O-2; Xylp-3^{II} means Xylp-3 branched at O-3; Xylp-3^{III} means Xylp-3 branched at O-2,3. [c] In p.p.m. relative to the signal of internal sodium 4,4-dimethyl-4-silapentane-1-sulfonate (using internal acetone at δ 2.225) in D$_2$O at 27°, acquired at 600 MHz. [d] The specific assignments are deduced from the ROESY spectrum of fractions **54** (A^{3X4} H-1,4^{II} H-3 of **AX-54c** and A^{3X4} H-1,4^{II} H-3 of **AX-54b**). [e] Each set of assignments may have to be interchanged.

residue were observed, and the data obtained are summarised in Table III. The essential part of the ROESY spectrum of the non-subfractionated fraction **54** is presented in Fig. 7 and the observed n.O.e.'s along the H-1 tracks are compiled in Table IV. The n.O.e.'s between H-1 of β-Xylp-(**n**) and H-4,5eq of β-Xylp-(**n** − **1**), together with the connectivities α-Araf-A^{2X3} H-1,β-Xylp-3^{III} H-2, α-Araf-A^{3X3} H-1,β-Xylp-3^{III} H-3, and α-Araf-A^{3X4} H-1,β-Xylp-4^{II} H-3, established the sequence of **AX-54c**.

A^{3X4}

α-Ara*f*–(1→3)

5   4^{II} 3^{III} 2   1

β-Xyl*p*–(1→4)–β-Xyl*p*–(1→4)–β-Xyl*p*–(1→4)–β-Xyl*p*–(1→4)–Xyl*p*

α-Ara*f*–(1→3)

A^{3X3} α-Ara*f*–(1→2)
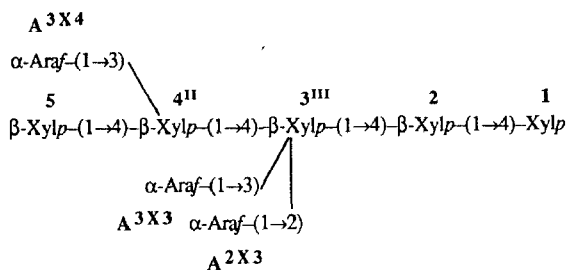
A^{2X3}

(AX-54c)

Besides these n.O.e.'s, the ROESY spectrum shows also the inter-residual connec-
tivities A^{2X3}-H-1,A^{3X3}-H-2 and A^{3X3}-H-1,A^{2X3}-H-2, characteristic for the 2,3-substitution
of a (1→4)-linked β-Xyl*p* by two terminal α-Ara*f* residues {see reference compound
AX-33 [β-Xyl*p*-4-(α-Ara*f*-A^{2X3})(α-Ara*f*-A^{3X3})β-Xyl*p*-3^{III}-β-Xyl*p*-2-Xyl*p*-1]^4}. Compari-
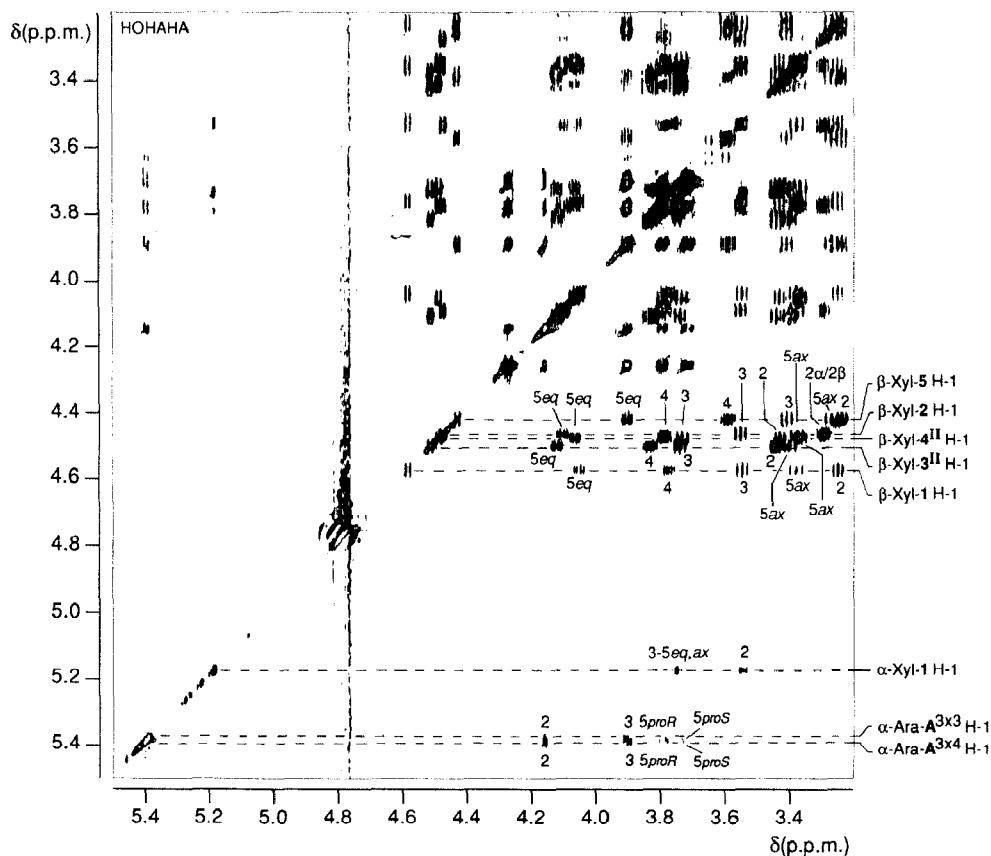

Fig. 4. 600-MHz HOHAHA spectrum of fraction **41**. Diagonal peaks of the anomeric protons are
indicated. The numbers near cross-peaks refer to the protons of the scalar-coupling network belonging to a
diagonal peak.

TABLE IV

Cross-peaks observed at the H-1 tracks in the ROESY spectra of arabinoxylan hepta- to tetradeca-saccharides, measured with a mixing time of 200 ms

Compound	Residue	N.O.e. effect
AX-41	Xyl-2 H-1	Xyl-2 H-3(very weak),5ax; Xyl-1β H-4
	Xyl-3^{II} H-1	Xyl-3^{II} H-3,5ax; Xyl-2 H-4,5eq
	Xyl-4^{II} H-1	Xyl-4^{II} H-3,5ax; Xyl-3^{II} H-4,5eq
	Xyl-5 H-1	Xyl-5 H-3(very weak),5ax; Xyl-4^{II} H-4,5eq
	Ara-A^{3X3} H-1	Ara-A^{3X3} H-2; Xyl-3^{II} H-3
	Ara-A^{3X4} H-1	Ara-A^{3X4} H-2; Xyl-4^{II} H-3
AX-54c	Xyl-2 H-1	Xyl-2 H-3,5ax; Xyl-1β H-4,5eq; Xyl-1α H-4,5
	Xyl-3^{III} H-1	Xyl-3^{III} H-3,5ax; Xyl-2 H-4,5eq
	Xyl-4^{II} H-1	Xyl-4^{II} H-3,5ax; Xyl-3^{III} H-4,5eq
	Xyl-5 H-1	Xyl-5 H-3,5ax; Xyl-4^{II} H-4,5eq
	Ara-A^{2X3} H-1	Ara-A^{2X3} H-2; Ara-A^{3X3} H-2; Xyl-3^{III} H-2
	Ara-A^{3X3} H-1	Ara-A^{3X3} H-2; Ara-A^{2X3} H-2; Xyl-3^{III} H-3
	Ara-A^{3X4} H-1	Ara-A^{3X4} H-2; Xyl-4^{II} H-3
AX-54b	Xyl-2 H-1	Xyl-2 H-3,5ax; Xyl-1β H-4,5eq; Xyl-1α H-4,5
	Xyl-3^{III} H-1	Xyl-3^{III} H-3,5ax; Xyl-2 H-4,5,eq
	Xyl-4^{II} H-1	Xyl-4^{II} H-3,5ax; Xyl-3^{III} H-4,5eq
	Xyl-5 H-1	Xyl-5 H-5ax; Xyl-4^{II} H-4(very weak),5eq
	Xyl-6 H-1	Xyl-6 H-3,5ax; Xyl-5 H-4,5eq
	Ara-A^{2X3} H-1	Ara-A^{2X3} H-2; Ara-A^{3X3} H-2; Xyl-3^{III} H-2
	Ara-A^{3X3} H-1	Ara-A^{3X3} H-2; Ara-A^{2X3} H-2; Xyl-3^{III} H-3
	Ara-A^{3X4} H-1	Ara-A^{3X4} H-2; Xyl-4^{II} H-3
AX-56	Xyl-2 H-1	Xyl-2 H-3(very weak),5ax; Xyl-1β H-4,5eq; Xyl-1α H-5
	Xyl-3^{II} H-1	Xyl-3^{II} H-3,5ax; Xyl-2 H-4,5eq
	Xyl-4^{III} H-1	Xyl-4^{III} H-3,5ax; Xyl-3^{II} H-4,5eq
	Xyl-5 H-1	Xyl-5 H-3,5ax; Xyl-4^{III} H-4,5eq
	Ara-A^{3X3} H-1	Ara-A^{3X3} H-2; Xyl-3^{II} H-3
	Ara-A^{2X4} H-1	Ara-A^{2X4} H-2; Ara-A^{3X4} H-2; Xyl-4^{III} H-2
	Ara-A^{3X4} H-1	Ara-A^{3X4} H-2; Ara-A^{2X4} H-2; Xyl-4^{III} H-3
AX-59	Xyl-2 H-1	Xyl-2 H-3(weak),5ax; Xyl-1β H-4,5eq; Xyl-1α H-5
	Xyl-3^{III} H-1	Xyl-3^{III} H-3,5ax; Xyl-2 H-4,5eq
	Xyl-4^{III} H-1	Xyl-4^{III} H-3,5ax; Xyl-3^{III} H-4,5eq
	Xyl-5 H-1	Xyl-5 H-3,5ax; Xyl-4^{III} H-4,5eq
	Ara-A^{2X3} H-1	Ara-A^{2X3} H-2; Ara-A^{3X3} H-2; Xyl-3^{III} H-2
	Ara-A^{3X3} H-1	Ara-A^{3X3} H-2; Ara-A^{2X3} H-2; Xyl-3^{III} H-3
	Ara-A^{2X4} H-1	Ara-A^{2X4} H-2; Ara-A^{3X4} H-2; Xyl-4^{III} H-2
	Ara-A^{3X4} H-1	Ara-A^{3X4} H-2; Ara-A^{2X4} H-2; Xyl-4^{III} H-3
AX-58a	Xyl-2 H-1	Xyl-2 H-5ax(weak); Xyl-1β H-4(weak)
	Xyl-3 H-1	Xyl-3 H-5ax; Xyl-2 H-4,5eq(weak)
	Xyl-4^{III} H-1	Xyl-4^{III} H-3,5ax; Xyl-3 H-4,5eq
	Xyl-5^{III} H-1	Xyl-5^{III} H-3,5ax; Xyl-4^{III} H-4,5eq
	Xyl-6 H-1	Xyl-6 H-5ax; Xyl-5^{III} H-4,5eq
	Ara-A^{2X4} H-1	Ara-A^{2X4} H-2; Ara-A^{3X4} H-2; Xyl-4^{III} H-2
	Ara-A^{3X4} H-1	Ara-A^{3X4} H-2; Ara-A^{2X4} H-2; Xyl-4^{III} H-3
	Ara-A^{2X5} H-1	Ara-A^{2X5} H-2; Ara-A^{3X5} H-2; Xyl-5^{III} H-2
	Ara-A^{3X5} H-1	Ara-A^{3X5} H-2; Ara-A^{2X5} H-2; Xyl-5^{III} H-3

TABLE IV (continued)

Compound	Residue	N.O.e. effect
AX-58b	Xyl-**2** H-1	Xyl-**2** H-3,5*ax*; Xyl-**1**β H-4,5*eq*; Xyl-**1**α H-4
	Xyl-**3**''' H-1	Xyl-**3**''' H-3,5*ax*; Xyl-**2** H-4,5*eq*
	Xyl-**4**''' H-1	Xyl-**4**''' H-3,5*ax*; Xyl-**3**''' H-4,5*eq*
	Xyl-**5** H-1	Xyl-**5** H-5*ax*; Xyl-**4**''' H-4,5*eq*
	Xyl-**6** H-1	Xyl-**6** H-3(weak),5*ax*; Xyl-**5** H-4,5*eq*
	Ara-A^{2X3} H-1	Ara-A^{2X3} H-2; Ara-A^{3X3} H-2; Xyl-**3**''' H-2
	Ara-A^{3X3} H-1	Ara-A^{3X3} H-2; Ara-A^{2X3} H-2; Xyl-**3**''' H-3
	Ara-A^{2X4} H-1	Ara-A^{2X4} H-2; Ara-A^{3X4} H-2; Xyl-**4**''' H-2
	Ara-A^{3X4} H-1	Ara-A^{3X4} H-2; Ara-A^{2X4} H-2; Xyl-**4**''' H-3
AX-57a	Xyl-**2** H-1	Xyl-**2** H-5*ax*; Xyl-**1**β H-4(weak),5*eq*(weak); Xyl-**1**α H-4(weak)
	Xyl-**3**''' H-1	Xyl-**3**''' H-5*ax*; Xyl-**2** H-4,5*eq*
	Xyl-**4** H-1	Xy-**4** H-3,5*ax*; Xyl-**3**''' H-4,5*eq*
	Xyl-**5**''' H-1	Xyl-**5**''' H-3,5*ax*; Xyl-**4** H-4,5*eq*
	Xyl-**6** H-1	Xyl-**6** H-3,5*ax*; Xyl-**5**''' H-4,5*eq*
	Ara-A^{2X3} H-1	Ara-A^{2X3} H-2; Ara-A^{3X3} H-2; Xyl-**3**''' H-2
	Ara-A^{3X3} H-1	Ara-A^{3X3} H-2; Ara-A^{2X3} H-2; Xyl-**3**''' or **5**''' H-3,4(very weak)^a
	Ara-A^{2X5} H-1	Ara-A^{2X5} H-2; Ara-A^{3X5} H-2; Xyl-**5**''' H-2
	Ara-A^{3X5} H-1	Ara-A^{3X5} H-2; Ara-A^{2X5} H-2; Xyl-**5**''' or **3**''' H-3,4(very weak)^a
AX-57b	Xyl-**2** H-1	Xyl-**2** H-3,5*ax*; Xyl-**1**β H-4,5*eq*; Xyl-**1**α H-4(weak)
	Xyl-**3**''' = **6**''' H-1	Xyl-**3**''' and **6**''' H-3,5*ax*; Xyl-**2** and **5** H-4,5*eq*
	Xyl-**4** H-1	Xyl-**4** H-3,5*ax*; Xyl-**3**''' H-4,5*eq*
	Xyl-**5** H-1	Xyl-**5** H-3,5*ax*; Xyl-**4** H-4,5*eq*
	Xyl-**7** H-1	Xyl-**7** H-3,5*ax*; Xyl-**6**''' H-4,5*eq*
	Ara-A$^{2|X3,X6|}$	Ara-A^2 H-2,3(very weak); Ara-A^3 H-2; Xyl-**3**''' and **6**''' H-2
	Ara-A$^{3|X3,X6|}$	Ara-A^3 H-2,3(very weak); Ara-A^2 H-2; Xyl-**3**''' and **6**''' H-3,4(weak)^a
AX-60	Xyl-**2** H-1	Xyl-**2** H-3,5*ax*; Xyl-**1**β H-4,5*eq*
	Xyl-**3**''' H-1	Xyl-**3**''' H-3,5*ax*; Xyl-**2** H-4,5*eq*
	Xyl-**4**''' H-1	Xyl-**4**''' H-3,5*ax*; Xyl-**3**''' H-4,5*eq*
	Xyl-**5** H-1	Xyl-**5** H-3,5*ax*; Xyl-**4**''' H-4,5*eq*
	Xyl-**6** H-1	Xyl-**6** H-3,5*ax*; Xyl-**5** H-4,5*eq*
	Xyl-**7**''' H-1	Xyl-**7**''' H-3,5*ax*; Xyl-**6** H-4,5*eq*
	Xyl-**8** H-1	Xyl-**8** H-3,5*ax*; Xyl-**7**''' H-4,5*eq*
	Ara-A^{2X3} H-1	Ara-A^{2X3} H-2; Ara-A^{3X3} H-2; Xyl-**3**''' H-2
	Ara-A^{3X3} H-1	Ara-A^{3X3} H-2; Ara-A^{2X3} H-2; Xyl-**3**''' H-3
	Ara-A^{2X4} H-1	Ara-A^{2X4} H-2; Ara-A^{3X4} H-2; Xyl-**4**''' H-2
	Ara-A^{3X4} H-1	Ara-A^{3X4} H-2; Ara-A^{2X4} H-2; Xyl-**4**''' H-3,4(very weak)^a
	Ara-A^{2X7} H-1	Ara-A^{2X7} H-2; Ara-A^{3X7} H-2; Xyl-**7**''' H-2
	Ara-A^{3X7} H-1	Ara-A^{3X7} H-2; Ara-A^{2X7} H-2; Xyl-**7**''' H-3

^{a} Cross-peak is a relayed ROESY contact, caused by spin diffusion due to the small chemical shift difference between H-3 and H-4 of the 2,3-branched β-Xyl*p*.

son of the ^{1}H-n.m.r. data of **AX-54c** with those of **AX-41** (Table III) and reference compound **AX-34b** [β-Xyl*p*-5-β-Xyl*p*-4-(α-Ara*f*-A^{2X3})(α-Ara*f*-A^{3X3})β-Xyl*p*-3'''-β-Xyl*p*-2-Xyl*p*-1][4] shows only small differences in chemical shift between the signals of the single-branched unit [(α-Ara*f*-A^{3X4})β-Xyl*p*-4''] of **AX-54c** and of **AX-41**, and between the signals of the double-branched unit [(α-Ara*f*-A^{2X3})(α-Ara*f*-A^{3X3})β-Xyl*p*-3'''] of **AX-54c** and of **AX-34b**.
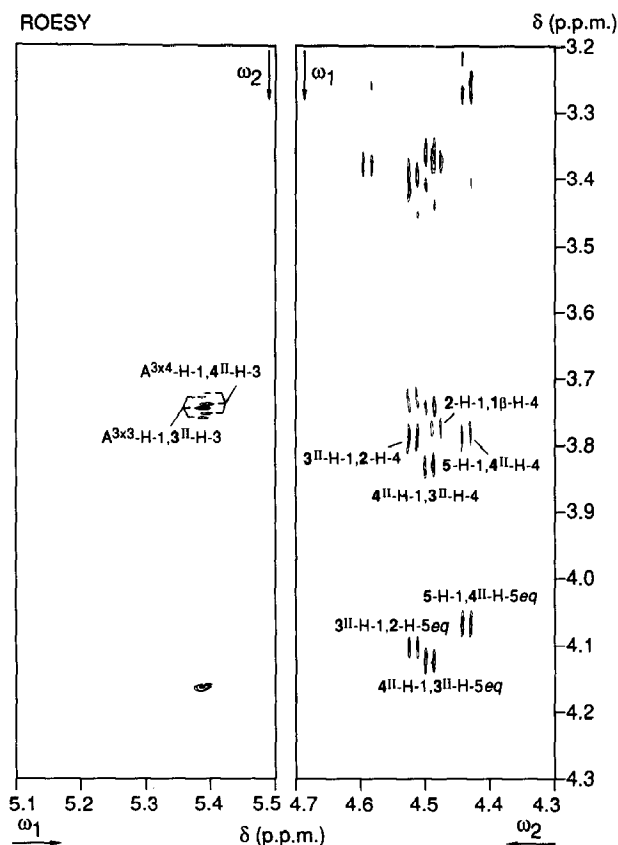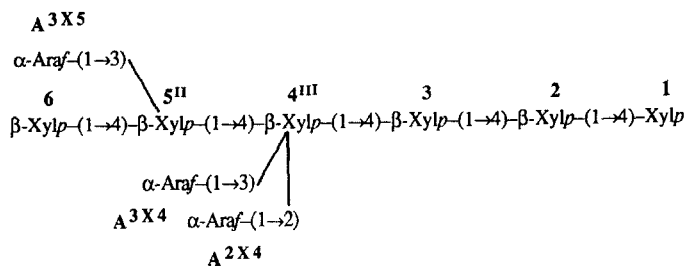
Fig. 5. 600-MHz ROESY spectrum of fraction **41**. N.O.e. connectivities are given along the H-1 tracks in the ω_1-dimension for the β-Xyl$p$ residues, and in the ω_2-dimension for the α-Ara$f$ residues. Only the inter-residual n.O.e. connectivities are denoted and only the negative levels are given. A^{3X3}-H-1,3^{II}-H-3 means the cross-peak between H-1 of α-Ara$f$-A^{3X3} and H-3 of β-Xyl$p$-3^{II}, etc.

Fraction **54.2**. — The data in Tables I and II indicate that **54.2** contained nonasaccharide(s) built up from a xylohexaose core with internal β-Xyl$p$ residues both 3- and 2,3-substituted by three α-Ara$f$. The intensities of the signals for anomeric protons in the ¹H-n.m.r. spectrum of fraction **54.2** (Fig. 6B) indicate the presence of a mixture of nonasaccharides. Two α-Ara$f$ H-1 signals are present at δ 5.402 and 5.396, with relative intensities of 1:2. In the region for anomeric protons of the ¹H-n.m.r. spectrum of **54.2**, the β-Xyl$p$ H-1 signals of **AX-54c** are observed, but the signal at δ 4.435 has a lower intensity. Also, additional β-Xyl$p$ H-1 signals are present at δ 4.479 (from HOHAHA data), 4.472, 4.453, and 4.448. The H-1 signal at δ 4.435 has the same order of magnitude as the α-Ara$f$ H-1 signal at δ 5.402. These signals, in combination with those at δ 4.637, 4.481, 5.225, and 5.270, indicate, for the minor triarabinosyl-xylohexaose (**AX-54a**), the same terminal sequence as in **AX-54c**, i.e., β-Xyl$p$-5-(α-Ara$f$-A^{3X4})β-Xyl$p$-4^{II}-(α-Ara$f$-A^{2X3})(α-Ara$f$-A^{3X3})β-Xyl$p$-3^{III}, denoted β-Xyl$p$-6-(α-Ara$f$-A^{3X5})-β-Xyl$p$-5^{II}-(α-Ara$f$-A^{2X4})(α-Ara$f$-A^{3X4})β-Xyl$p$-4^{III} in structure **AX-54a** (see below). The

connection of this terminal sequence to a reducing xylotriose unit is supported by the observation of the H-1 signals at δ 4.472 (β-Xyl$p$-3) and 4.479 (β-Xyl$p$-2), which match completely the H-1 signals of β-Xyl$p$-3 and β-Xyl$p$-2 of reference compound **AX-34a** [β-Xyl$p$-5-(α-Ara$f$-A^{2X4})(α-Ara$f$-A^{3X4})β-Xyl$p$-4^{III}-β-Xyl$p$-3-β-Xyl$p$-2-Xyl$p$-1][4], with an identical diarabinosylxylotetraosyl reducing element. Based on the combined ^{1}H-n.m.r. data, the structure of the minor component of **54.2** is

A^{3X5}

α-Ara$f$-(1→3)

```
       6            5^II           4^III          3            2            1
β-Xylp-(1→4)-β-Xylp-(1→4)-β-Xylp-(1→4)-β-Xylp-(1→4)-β-Xylp-(1→4)-Xylp
```

α-Ara$f$-(1→3)

A^{3X4} α-Ara$f$-(1→2)

A^{2X4}

(AX-54a)

The major triarabinosylxylohexaose **AX-54b** contained a terminal unbranched xylobiosyl unit at the non-reducing end, characterised by the H-1 signals at δ 4.448 and 4.453 for the terminal and penultimate β-Xyl$p$ residues, respectively (Table III). The ROESY data of **54** (Fig. 7 and Table IV) show that the β-Xyl$p$ H-1 signal at δ 4.448 has a cross-peak with H-4,5eq of the β-Xyl$p$ residue with H-1 at δ 4.453. Furthermore, the β-Xyl$p$ H-1 resonance at δ 4.453 has a cross-peak with H-4,5eq of a 3-branched β-Xyl$p$ residue, whereas the intensities of the β-Xyl$p$ H-1 signals at δ 4.448 and 4.453 are
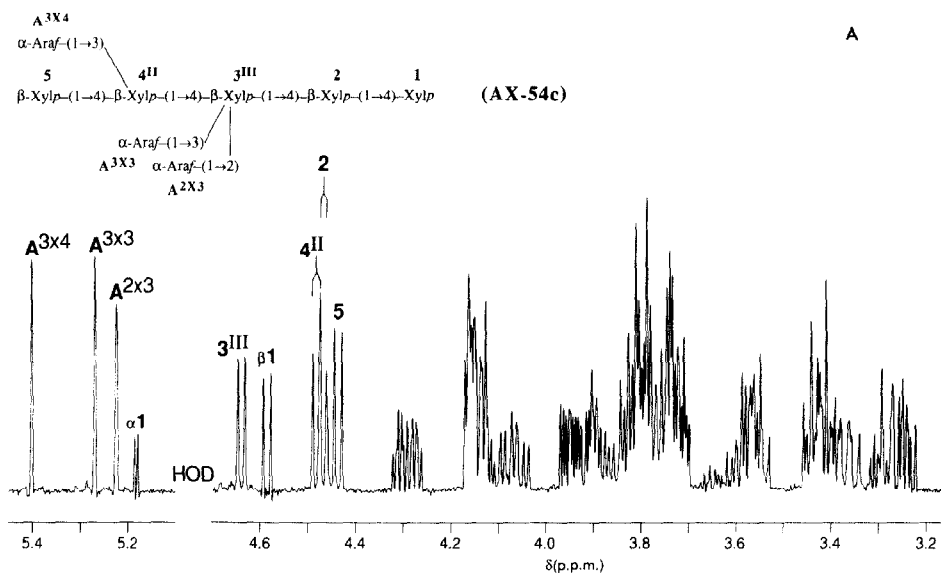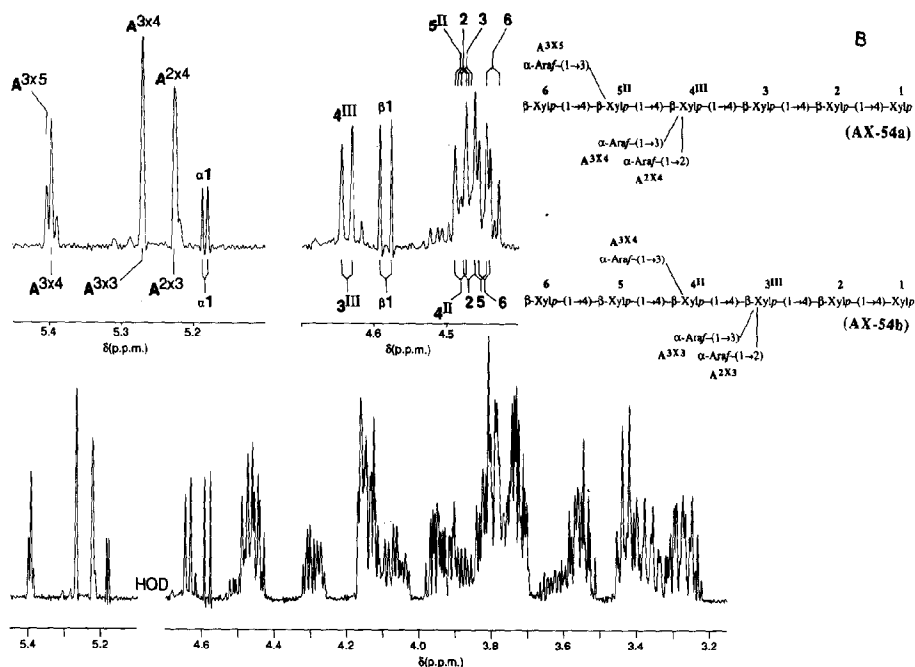
Fig. 6. Resolution-enhanced 600-MHz ¹H-n.m.r. spectra of fractions **54.3** (A) and **54.2** (B). The numbers and letters in the spectrum refer to the corresponding residues in the structure.

comparable to that of the α-Ara$f$ H-1 signal at δ 5.396. Combination of these data leads to the terminal sequence β-Xyl$p$-**6**-β-Xyl$p$-**5**-(α-Ara$f$-A^{3X4})β-Xyl$p$-**4^{II}** for **AX-54b** (see also the cross-peak A^{3X4}-H-1,4^{II}-H-3). The H-1 signals of β-Xyl$p$-**1,2** resonate at the same values as those of the corresponding residues in **AX-54c**. The same holds for the remaining 2,3-substituted β-Xyl$p$ residue, which connects the discussed non-reducing and reducing elements, resulting in structure **AX-54b**.
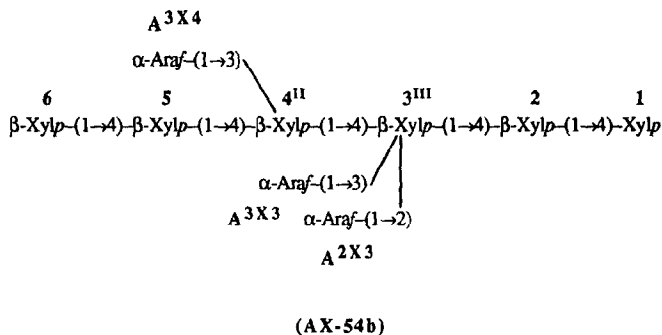
In Fig. 6B, signals were also observed of a third compound of which the structure could not be unravelled, due to the still lower amount of material.

Fig. 7. 600-MHz ROESY spectrum of fraction **54**. N.O.e. connectivities are given along the H-1 tracks in the ω_1-dimension for the β-Xyl$p$ residues, and in the ω_2-dimension for the α-Ara$f$ residues. Only the inter-residual n.O.e. connectivities are denoted and only the negative levels are given. The specific n.O.e. connectivities of **AX-54b** are given between square brackets. A^{3X4}-H-1,4^{II}-H-3 means the cross-peak between H-1 of α-Ara$f$-A^{3X4} and H-3 of β-Xyl$p$-4^{II}, *etc.*

Fraction **56**. — The intensities of the signals for anomeric protons in the ^{1}H-n.m.r. spectrum of **56** (Fig. 8) indicated the presence of a triarabinosylxylopentaose, **AX-56**, as the major compound. On the various H-1 tracks of the constituent monosaccharides in the 2D HOHAHA spectrum (not shown), the total scalar-coupled networks of each residue were observed, and the data obtained are summarised in Table III. Part of the ROESY spectrum is presented in Fig. 9 and the observed n.O.e.'s along the H-1 tracks are compiled in Table IV. The n.O.e.'s between H-1 of β-Xyl$p$-(n) and H-4,5eq of β-Xyl$p$-(n – 1), together with the connectivities α-Ara$f$-A^{3X3} H-1,β-Xyl$p$-3^{II} H-3, α-Ara$f$-A^{2X4} H-1,β-Xyl$p$-4^{III} H-2, and α-Ara$f$-A^{3X4} H-1,β-Xyl$p$-4^{III} H-3 established the sequence of **AX-56**. In addition, the inter-residual A^{2X4} H-1,A^{3X4} H-2 and A^{3X4} H-1,A^{2X4} H-2 connectivities, characteristic for the 2,3-substitution of an internal β-Xyl$p$ by two α-Ara$f$ residues, were observed.

A^{2X4}

A^{3X4} α-Araf-(1→2)

α-Araf-(1→3)

5   4ᴵᴵᴵ   3ᴵᴵ   2   1

β-Xylp-(1→4)-β-Xylp-(1→4)-β-Xylp-(1→4)-β-Xylp-(1→4)-Xylp

α-Araf-(1→3)

A^{3X3}

(AX-56)

Compound **AX-56** is an extension of **AX-41** with one α-Araf residue in (1→2) linkage to β-Xylp-4 (4ᴵᴵ→4ᴵᴵᴵ). Comparison of the ¹H-n.m.r. data of **AX-56** with those of **AX-41** (Table III) shows for **AX-56** downfield shifts of the α-Araf-A^{3X3} protons, except H-2. The conversion of β-Xylp-4ᴵᴵ into β-Xylp-4ᴵᴵᴵ is also accompanied by downfield shifts for this residue, whereby the downfield shift of H-3 to δ 3.80 results in overlap with the H-4 signal. Comparison of the ¹H-n.m.r. data of the two triarabinosylxylopentaoses **AX-56** and **AX-54c** shows specific differences, which directly reflect the distribution of the three α-Araf residues over the internal xylobiose residue (see, *e.g.*, the H-1 signals of β-Xylp-3ᴵᴵ *versus* -3ᴵᴵᴵ, and of β-Xylp-4ᴵᴵ *versus* -4ᴵᴵᴵ).

The spectrum in Fig. 8 shows the presence of two minor β-Xylp H-1 signals at δ 4.441 and 4.449, demonstrating that one of the minor oligosaccharides of **56** has a
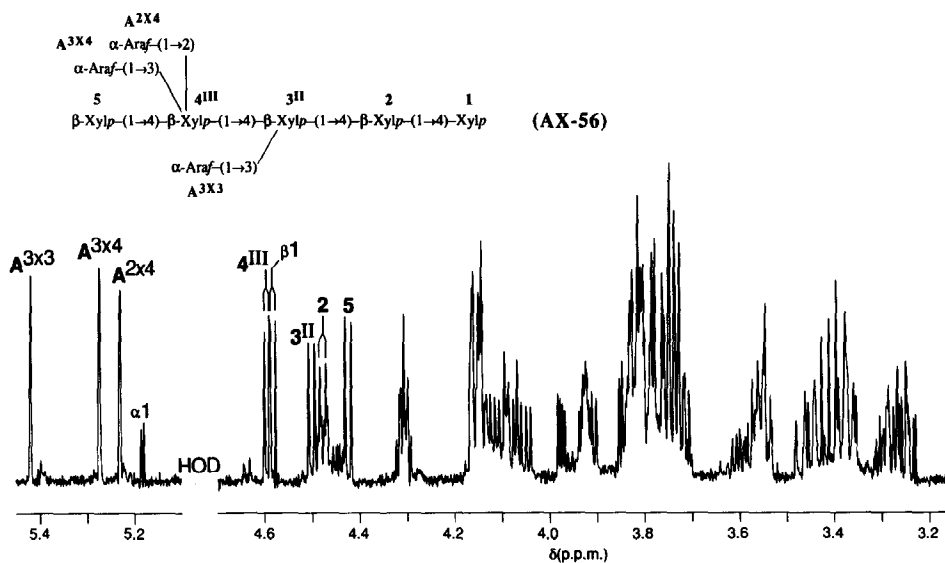
Fig. 8. Resolution-enhanced 600-MHz ¹H-n.m.r. spectrum of fraction **56**. The numbers and letters in the spectrum refer to the corresponding residues in the structure.
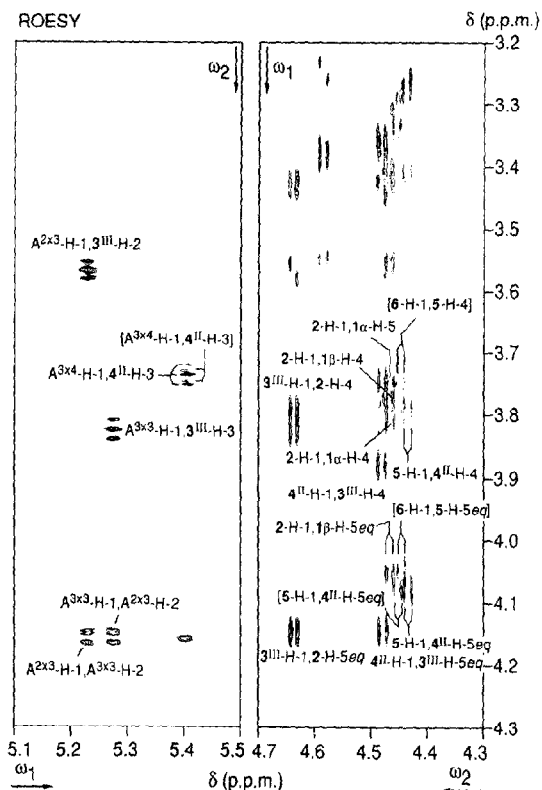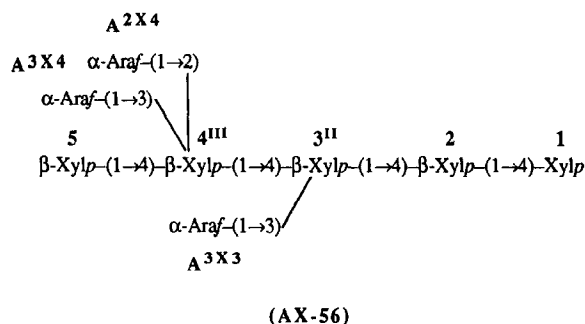
Fig. 9. 600-MHz ROESY spectrum of fraction **56**. N.O.e. connectivities are given along the H-1 tracks in the ω_1-dimension for the β-Xyl*p* residues, and in the ω_2-dimension for the α-Ara*f* residues. Only the inter-residual n.O.e. connectivities are denoted and only the negative levels are given. A^{3X3}-H-1,3^{II}-H-3 means the cross-peak between H-1 of α-Ara*f*-A^{3X3} and H-3 of β-Xyl*p*-3^{II}, *etc.*

terminal unbranched xylobiosyl unit, presumably 4-linked to a 2,3-branched β-Xyl*p* residue (see **AX-58b**, Table III).

Fraction **59**. — The intensities of the signals for anomeric protons in the ^{1}H-n.m.r. spectrum of **59** (Fig. 10A) indicated the presence of a tetra-arabinosylxylopentaose, **AX-59**. On the various H-1 tracks of the constituent monosaccharides in the 2D HOHAHA spectrum (not shown), the total scalar-coupled networks of each residue were observed, and the data obtained are summarised in Table III. The observed n.O.e.'s along the H-1 tracks in the ROESY spectrum (not shown) are compiled in Table IV. The n.O.e.'s between H-1 of β-Xyl*p*-**(n)** and H-4,5*eq* of β-Xyl*p*-**(n - 1)**, together with the connectivities α-Ara*f*-A^{2X3} H-1,β-Xyl*p*-3^{III} H-2, α-Ara*f*-A^{3X3} H-1,β-Xyl*p*-3^{III} H-3, α-Ara*f*-A^{2X4} H-1,β-Xyl*p*-4^{III} H-2, and α-Ara*f*-A^{3X4} H-1,β-Xyl*p*-4^{III} H-3, establish the sequence of **AX-59**. The presence of the tetra-arabinosylxylobiose residue in **AX-59** is reflected by a characteristic set of four α-Ara*f* H-1 signals (Table III). It is noteworthy

Fig. 10. Resolution-enhanced 600-MHz ¹H-n.m.r. spectra of fractions **59** (A) and **58** (B). The numbers and letters in the spectrum refer to the corresponding residues in the structure.
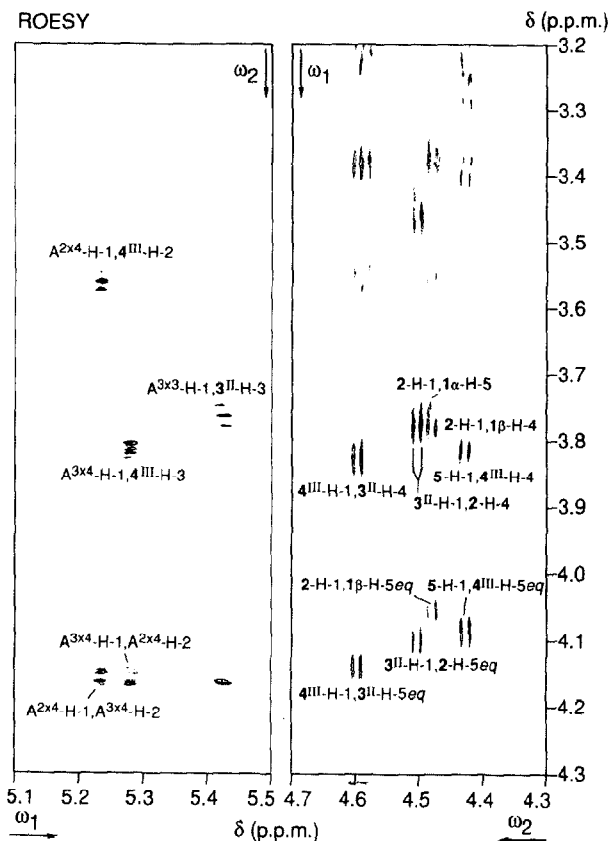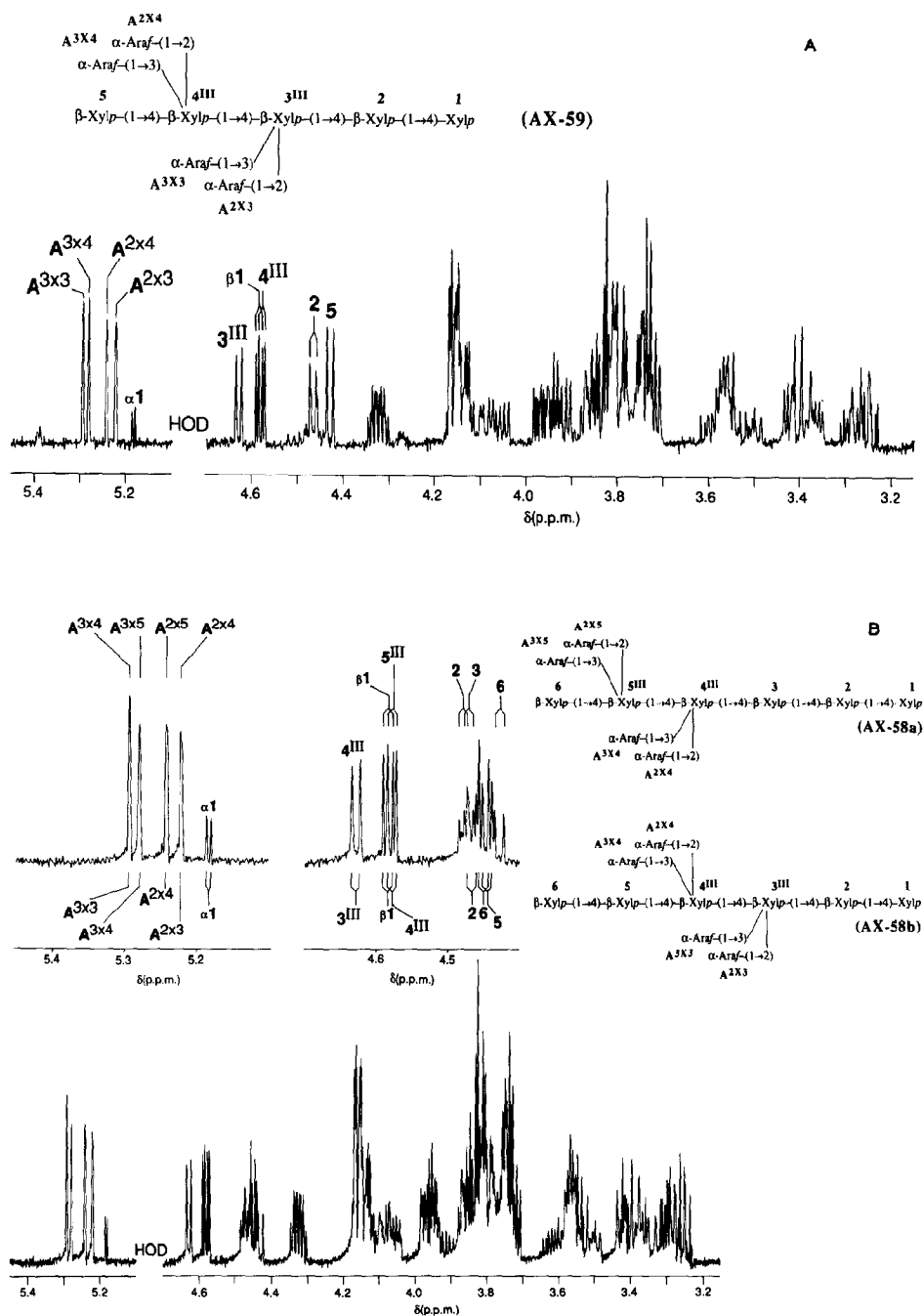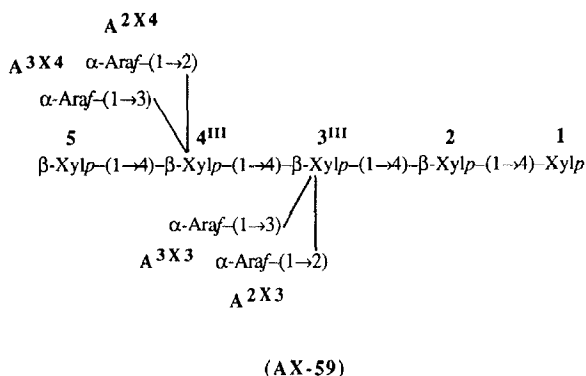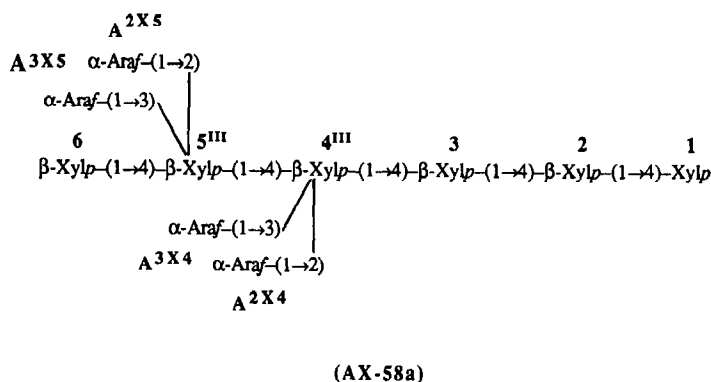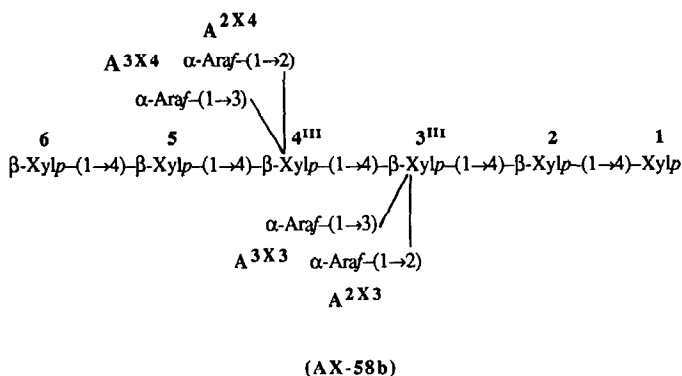
that the inter-residual α-Ara$f$ H-1,2 connectivities between α-Ara$f$-A^{2X3} and α-Ara$f$-A^{3X3} and between α-Ara$f$-A^{2X4} and α-Ara$f$-A^{3X4} support the presence of two 2,3-branched β-Xyl$p$ residues.

$$
\begin{array}{l}
\text{A}^{2X4} \\
\text{A}^{3X4} \quad \alpha\text{-Araf-}(1\rightarrow2) \\
\quad \alpha\text{-Araf-}(1\rightarrow3) \\
\quad\quad 5 \qquad\qquad 4^{\text{III}} \qquad\qquad 3^{\text{III}} \qquad\qquad 2 \qquad\qquad 1 \\
\beta\text{-Xylp-}(1\rightarrow4)\text{-}\beta\text{-Xylp-}(1\rightarrow4)\text{-}\beta\text{-Xylp-}(1\rightarrow4)\text{-}\beta\text{-Xylp-}(1\rightarrow4)\text{-Xylp} \\
\quad\quad\quad \alpha\text{-Araf-}(1\rightarrow3) \\
\quad\quad \text{A}^{3X3} \quad \alpha\text{-Araf-}(1\rightarrow2) \\
\quad\quad\quad \text{A}^{2X3}
\end{array}
$$

(AX-59)

Fraction **58**. — The data presented in Tables I and II indicate that **58** contained decasaccharide(s) built up from a xylohexaose core with two internal β-Xyl$p$ residues 2,3-substituted by four α-Ara$f$. The ^{1}H-n.m.r. spectrum of **58** (Fig. 10B) contains signals with different intensities which indicate that two decasaccharides were present. The ratio was determined to be 1:2, based on the relative intensities of the two H-1 signals of terminal β-Xyl$p$ residues at δ 4.429 and 4.450, respectively. In the region for anomeric protons, the characteristic set of α-Ara$f$ H-1 signals, indicating a tetra-arabinosyl-xylobiose element (see **AX-59**), were present. Furthermore, the β-Xyl$p$ H-1 signals of **AX-59** were observed; however, they differ in intensities. Besides these β-Xyl$p$ H-1 resonances, additional ones at δ 4.471, 4.478, 4.445, and 4.450 were present. The signals at δ 4.471 and 4.478 have the same order of magnitude as the β-Xyl$p$ H-1 signal at δ 4.429. In **AX-59**, δ 4.429 corresponds to the non-reducing terminal β-Xyl$p$ residue, connected to the tetra-arabinosylxylobiose element. Combined HOHAHA and ROE-SY data (Tables III and IV, respectively) indicated that the terminal heptasaccharide in **AX-59**, *i.e.*, β-Xyl$p$-5-(α-Ara$f$-A^{2X4})(α-Ara$f$-A^{3X4})β-Xyl$p$-4$^{\text{III}}$-(α-Ara$f$-A^{2X3})(α-Ara$f$-A^{3X3})-β-Xyl$p$-3$^{\text{III}}$, was also present in the minor tetra-arabinosylxylohexaose **AX-58a** in **58**, denoted β-Xyl$p$-6-(α-Ara$f$-A^{2X5})(α-Ara$f$-A^{3X5})β-Xyl$p$-5$^{\text{III}}$-(α-Ara$f$-A^{2X4})(α-Ara$f$-A^{3X4})β-Xyl$p$-4$^{\text{III}}$ (see below). These data also show that this non-reducing unit was extended with a xylotriose residue. In particular, the n.O.e. contacts β-Xyl$p$-4$^{\text{III}}$ H-1,β-Xyl$p$-3 H-4,5eq corroborate this conclusion. The H-1 signals at δ 4.471 and 4.478 are attributed to β-Xyl$p$-3 and β-Xyl$p$-2 H-1, respectively. The ^{1}H-n.m.r. resonances of β-Xyl$p$-3, except H-4, and β-Xyl$p$-2 have comparable chemical shifts as those of β-Xyl$p$-3 and β-Xyl$p$-2 of reference **AX-34a**[4], with an identical reducing structural element (α-Ara$f$-A^{2X4})(α-Ara$f$-A^{3X4})β-Xyl$p$-4$^{\text{III}}$-β-Xyl$p$-3-β-Xyl$p$-2-Xyl$p$-1. Based on the ^{1}H-n.m.r. data, the structure of **AX-58a** is

```
                    2X5
                   A
     A3X5   α-Araf-(1→2)
        α-Araf-(1→3)
           6        5ᴵᴵᴵ        4ᴵᴵᴵ        3         2         1
     β-Xylp-(1→4)-β-Xylp-(1→4)-β-Xylp-(1→4)-β-Xylp-(1→4)-β-Xylp-(1→4)-Xylp

              α-Araf-(1→3)
           A3X4  α-Araf-(1→2)
                  A2X4
```

(AX-58a)

The major tetra-arabinosylxylohexaose **AX-58b** contained at the non-reducing end an unbranched xylobiosyl unit, characterised by the H-1 signals at δ 4.450 and 4.445 for the terminal and penultimate β-Xylp residues, respectively (Table III). The ROESY data (Table IV) show that the H-1 signal at δ 4.445 has a cross-peak with H-4,5eq of the 2,3-branched β-Xylp residue, coded **4ᴵᴵᴵ** in **AX-58b** (see below). Thus, this terminal xylobiosyl unit was 4-linked to the internal tetra-arabinosylxylobiose residue. The signals of β-Xylp-**1,2** have the same chemical shifts as those of the corresponding residues in **AX-59**. Based on the combined ¹H-n.m.r. data, the structure of **AX-58b** is


```
                    2X4
                   A
     A3X4   α-Araf-(1→2)
        α-Araf-(1→3)
           6        5        4ᴵᴵᴵ       3ᴵᴵᴵ       2         1
     β-Xylp-(1→4)-β-Xylp-(1→4)-β-Xylp-(1→4)-β-Xylp-(1→4)-β-Xylp-(1→4)-Xylp

              α-Araf-(1→3)
           A3X3  α-Araf-(1→2)
                  A2X3
```

(AX-58b)

Fraction **57.2.** — The intensities of the signals for anomeric protons in the ¹H-n.m.r. spectrum of **57.2** (Fig. 11) indicated the presence of a tetra-arabinosyl-xylohexaose, **AX-57a**. On the various H-1 tracks of the constituent monosaccharides in the 2D HOHAHA spectrum (not shown), the total scalar-coupled networks of each residue were observed, and the data obtained are summarised in Table III. The observed n.O.e.'s along the H-1 tracks in the ROESY spectrum (not shown) are compiled in Table IV. The n.O.e.'s between H-1 of β-Xylp-(**n**) and H-4,5eq of β-Xylp-(**n** − **1**), together with the connectivities α-Araf-A^{2X3} H-1,β-Xylp-3ᴵᴵᴵ H-2, α-Araf-A^{3X3} H-1,β-Xylp-3ᴵᴵᴵ H-3, α-Araf-A^{2X5} H-1,β-Xylp-5ᴵᴵᴵ H-2, and α-Araf-A^{3X5} H-1,β-Xylp-5ᴵᴵᴵ H-3, established the sequence of **AX-57a**.

```
        6           5ᴵᴵᴵ         4          3ᴵᴵᴵ        2          1
β-Xylp-(1→4)-β-Xylp-(1→4)-β-Xylp-(1→4)-β-Xylp-(1→4)-β-Xylp-(1→4)-Xylp
                /      |                /      |
     α-Araf-(1→3)      |     α-Araf-(1→3)      |
A³ˣ⁵   α-Araf-(1→2)   A³ˣ³   α-Araf-(1→2)
        A²ˣ⁵                   A²ˣ³
```

(AX-57a)

It is noteworthy that already the set of chemical shifts of the four α-Araf H-1 signals excludes the presence of a tetra-arabinosylxylobiose unit. Furthermore, the H-1 signals of the two 2,3-branched β-Xylp residues separated by one unbranched β-Xylp residue had different chemical shifts (β-Xylp-3ᴵᴵᴵ H-1, δ 4.639 and β-Xylp-5ᴵᴵᴵ H-1, δ 4.628).

Fraction **57.1**. — The data in Tables I and II indicate that **57.1** contained xyloheptaose(s) with two internal β-Xylp residues 2,3-substituted by four α-Araf. The region for anomeric protons of the ^{1}H-n.m.r. spectrum of **57.1** (Fig. 12) contained signals with different intensities, indicating the presence of a mixture. The major undecamer, **AX-57b**, contained two 2,3-branched segments, (α-Araf-A²)(α-Araf-A³)β-Xylp, having comparable chemical shift values with those of the same segment in reference compound **AX-33** (ref. 4). The ^{1}H-n.m.r. data of these segments showed that, in the major compound, the two branched β-Xylp residues are separated by at least an unbranched xylobiose residue, since the ^{1}H-n.m.r. characteristics of a tetra-arabinosyl-xylobiose element (**AX-59**) and an element with two 2,3-substituted β-Xylp residues separated by one unbranched β-Xylp residue (**AX-57a**) are different. The HOHAHA

```
        6           5ᴵᴵᴵ         4          3ᴵᴵᴵ        2          1
β-Xylp-(1→4)-β-Xylp-(1→4)-β-Xylp-(1→4)-β-Xylp-(1→4)-β-Xylp-(1→4)-Xylp      (AX-57a)
               /      |               /      |
    α-Araf-(1→3)      |    α-Araf-(1→3)      |
A³ˣ⁵   α-Araf-(1→2)  A³ˣ³   α-Araf-(1→2)
        A²ˣ⁵                  A²ˣ³
```


Fig. 11. Resolution-enhanced 600-MHz ^{1}H-n.m.r. spectrum of fraction **57.2**. The numbers and letters in the spectrum refer to the corresponding residues in the structure.

Fig. 12. Resolution-enhanced 600-MHz ¹H-n.m.r. spectrum of fraction **57.1**. The numbers and letters in the spectrum refer to the corresponding residues in the structure.

and ROESY data (Tables III and IV, respectively) show that the β-Xylp H-1 signals at δ 4.436 and 4.639 correspond with a terminal sequence β-Xylp-7-(α-Araf-A^{2X6})(α-Araf-A^{3X6})β-Xylp-6ᴵᴵᴵ for **AX-57b** (see below) [compare with **AX-33** (ref.4)]. The ROESY data demonstrate (Table IV) that this terminal sequence was linked to an unbranched xylobiose residue, reflected by the β-Xylp H-1 signals at δ 4.454 (β-Xylp-**4**) and 4.463 (β-Xylp-**5**) (Table III). The β-Xylp H-1 signal at δ 4.454 has a cross-peak with H-4,5eq of a 2,3-branched β-Xylp residue, which can only be β-Xylp-3ᴵᴵᴵ (see below), connecting the internal xylobiose residue to the second branched residue. The signals of β-Xylp-**1,2** have the same chemical shifts as those of the corresponding residues in **AX-57a**. Based on the combined ¹H-n.m.r. data, the structure of **AX-57b** can be proposed as

(AX-57b)

Besides the H-1 signals attributed to **AX-57b**, a series of minor resonances of anomeric protons can be detected in the n.m.r. spectrum of **57.1**, namely, five β-Xylp H-1 doublets at δ 4.443, 4.452 (HOHAHA spectrum), 4.472, 4.479, and 4.628, and one

α-Ara*f* H-1 signal at δ 5.221. Combination of the β-Xyl*p* and α-Ara*f* H-1 signals at δ 4.443/4.628 and 5.221, together with β-Xyl*p* and α-Ara*f* H-1 signals at δ 4.639 and 5.226/5.273, already used for the characterisation of **AX-57b**, suggests the presence of an element with two 2,3-branched β-Xyl*p* residues, separated by one unbranched β-Xyl*p* residue, as in **AX-57a**. The β-Xyl*p* H-1 resonances at δ 4.472 and δ 4.479 can be attributed to β-Xyl*p*-3 and β-Xyl*p*-2 of a reducing xylotriose unit as in reference compound **AX-34a**. The β-Xyl*p* H-1 signal at δ 4.452 can be assigned to a terminal β-Xyl*p* residue of an unbranched xylobiosyl unit 4-linked to a 2,3-branched β-Xyl*p* residue, as in reference compound **AX-34b**[4] (penultimate β-Xyl*p* H-1, δ 4.454). However, in view of the complexity of the mixture, structures for the minor component(s) are not proposed.

Fraction **60**. — The data in Tables I and II indicate that **60** contained tetradeca-saccharide(s) built up from a xylo-octaose core with three internal β-Xyl*p* residues 2,3-substituted by six α-Ara*f*. The intensities of the signals for anomeric protons in the ^{1}H-n.m.r. spectrum of **60** (Fig. 13) indicated the presence of a hexa-arabinosylxylo-octaose, **AX-60**. Comparison of the ^{1}H-n.m.r. data of **AX-60** and **AX-58b** (Table III) shows that the ^{1}H-n.m.r. signals of the reducing terminal sequence β-Xyl*p*-5-(α-Ara*f*-A^{2X4})(α-Ara*f*-A^{3X4})β-Xyl*p*-4^{III}-(α-Ara*f*-A^{2X3})(α-Ara*f*-A^{3X3})β-Xyl*p*-3^{III}-β-Xyl*p*-2-Xyl*p*-1 of **AX-58b** are present in the spectrum of **AX-60**. Furthermore, the signals of a non-reducing terminal sequence β-Xyl*p*-(α-Ara*f*-A^2)(α-Ara*f*-A^3)β-Xyl*p*-β-Xyl*p*, as in
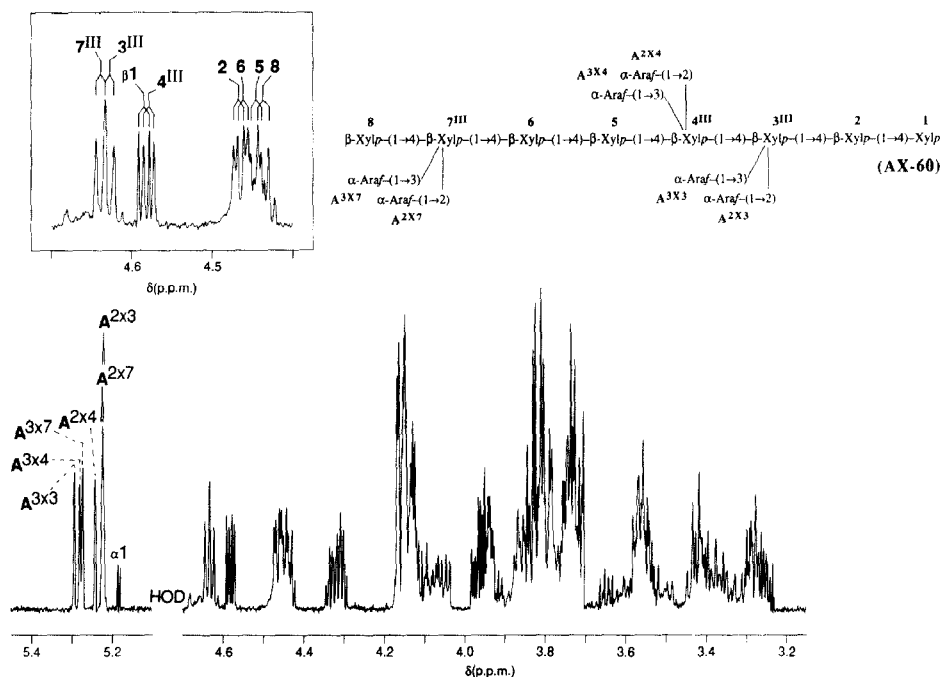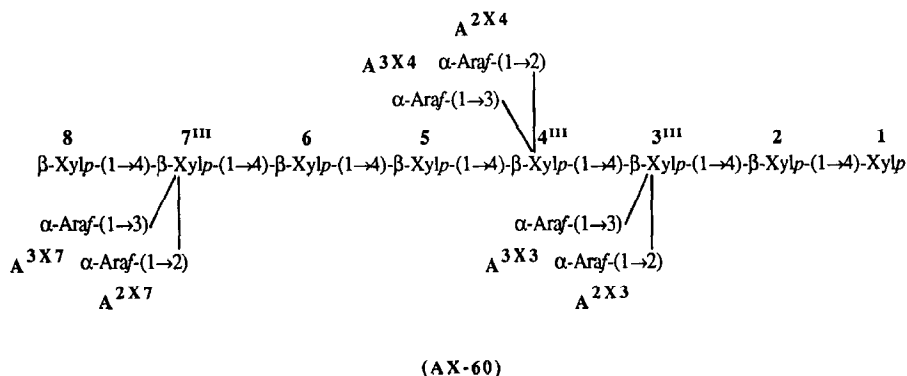

Fig. 13. Resolution-enhanced 600-MHz ^{1}H-n.m.r. spectrum of fraction **60**. The numbers and letters in the spectrum refer to the corresponding residues in the structure.

AX-57b, were detectable for **AX-60**. ROESY data (Table IV) show that the β-Xyl$p$ H-1 signal at δ 4.462 (β-Xyl$p$-6) has a cross-peak with H-4,5eq of β-Xyl$p$-5, establishing the sequence of **AX-60**.

(AX-60)

CONCLUDING REMARKS

In this and the previous[4] study, the primary structure of a series of arabinoxylan oligosaccharides, obtained by *Aspergillus* endo-($1\to4$)-β-D-xylanase digestion of wheat-endosperm arabinoxylan, has been determined. ¹H-N.m.r. spectroscopy, in combination with monosaccharide analysis, methylation analysis, and molecular mass determination (f.a.b.-m.s.), has been shown to be an excellent approach for the structural elucidation of this type of oligosaccharide. Owing to the characteristic positions of the H-1 resonances in relation to the various branching patterns in arabinoxylans, these n.m.r. data are suitable for the development of a structural-reporter-group concept. The data can be applied not only for the characterisation of arabinoxylans, but also for the study of substrate specificity of endo-($1\to4$)-β-D-xylanases from different biological sources.

An evaluation of the established structures shows the presence of the two elements $\to4$)[α-L-Ara$f$-($1\to3$)]-β-D-Xyl$p$-($1\to$ and/or $\to4$)[α-L-Ara$f$-($1\to2$)][α-L-Ara$f$-($1\to3$)]-β-D-Xyl$p$-($1\to$ directly connected to each other in all four possible combinations. The double-branched elements also occur separated by one or two unbranched β-Xyl$p$ residues. Furthermore, the oligosaccharides have, at the non-reducing end, one of two unbranched ($1\to4$)-linked β-Xyl$p$ residues, and at the reducing end two or three unbranched ($1\to4$)-linked β-Xyl$p$ residues. Based on these findings, it can be suggested that the minimum epitope for binding and cleavage of wheat arabinoxylans by the endo-($1\to4$)-β-D-xylanase from the *Aspergillus* species used consists of at least three unbranched ($1\to4$)-linked β-Xyl$p$ residues, whereby the type of branching seems to have no influence on the specificity of the enzymic cleavage. This means also that, in the native arabinoxylan, individual or clusters of branched elements are separated from each other by up to four unbranched β-Xyl$p$ residues, but, in view of the enzyme specificity, the occurrence of longer unbranched β-Xyl$p$ oligomers cannot be excluded.

REFERENCES

1 D. G. Medcalf and K. A. Gilles, *Cereal Chem.*, 45 (1968) 550 556.
2 R. A. Hoffmann, M. Roza, J. Maat, J. P. Kamerling, and J. F. G. Vliegenthart, *Carbohydr. Polym.*, 16 (1991) 275–289.
3 G. O. Aspinall and K. M. Ross, *J. Chem. Soc.*, (1963) 1681–1686.
4 R. A. Hoffmann, B. R. Leeflang, M. M. J. de Barse, J. P. Kamerling, and J. F. G. Vliegenthart, *Carbohydr. Res.*, 221 (1991) 63–81.
5 S. Huges and D. C. Johnson, *Anal. Chim. Acta*, 132 (1981) 11–22.
6 J. P. Kamerling and J. F. G. Vliegenthart, *Cell Biol. Monogr.*, 10 (1982) 95–125.
7 J. P. Kamerling, G. J. Gerwig, J. F. G. Vliegenthart, and J. R. Clamp, *Biochem. J.*, 151 (1975) 491–495.
8 A. L. Kvernheim, *Acta Chem. Scand., Ser. B*, 41 (1987) 150–152.
9 J. F. G. Vliegenthart, L. Dorland, and H. van Halbeek, *Adv. Carbohydr. Chem. Biochem.*, 41 (1983) 209–374.
10 A. Bax and D. G. Davis, *J. Magn. Reson.*, 65 (1985) 355–360.
11 L. Braunsweiler and R. R. Ernst, *J. Magn. Reson.*, 53 (1983) 521–526.
12 D. G. Davis and A. Bax, *J. Am. Chem. Soc.*, 107 (1985) 2820–2821.
13 M. W. Edwards and A. Bax, *J. Am. Chem. Soc.*, 108 (1986) 918–923.
14 A. Bax and D. G. Davis, *J. Magn. Reson.*, 63 (1985) 207–213.
15 D. Marion and K. Wüthrich, *Biochem. Biophys. Res. Commun.*, 113 (1983) 967–974.
16 M. M. Smith and R. D. Hartley, *Carbohydr. Res.*, 118 (1983) 65–80.
17 G. D. Wu, A. S. Serianni, and R. Baker, *J. Org. Chem.*, 48 (1983) 1750–1757.